Efficient realization of quantum algorithms with qudits

A.S. Nikolaeva, ^{1,2,3} E.O. Kiktenko, ^{1,2,4,3} and A.K. Fedorov^{1,3}

¹Russian Quantum Center, Skolkovo, Moscow 143025, Russia ²Moscow Institute of Physics and Technology, Moscow Region 141700, Russia ³National University of Science and Technology "MISIS", Moscow 119049, Russia ⁴Department of Mathematical Methods for Quantum Technologies, Steklov Mathematical Institute of Russian Academy of Sciences, Moscow 119991, Russia (Dated: June 22, 2022)

The development of a universal fault-tolerant quantum computer that can solve efficiently various difficult computational problems is an outstanding challenge for science and technology. In this work, we propose a technique for an efficient implementation of quantum algorithms with multilevel quantum systems (qudits). Our method uses a transpilation of a circuit in the standard qubit form, which depends on the parameters of a qudit-based processor, such as their number and the number of accessible levels. This approach provides a qubit-to-qudit mapping and comparison to a standard realization of quantum algorithms highlighting potential advantages of qudits. We provide an explicit scheme of transpiling qubit circuits into sequences of single-qudit and two-qudit gates taken from a particular universal set. We then illustrate our method by considering an example of an efficient implementation of a 6-qubit quantum algorithm with qudits. We expect that our findings are of relevance for ongoing experiments with noisy intermediate-scale quantum devices that operate with information carrier allowing qudit encodings, such as trapped ions and neutral atoms as well as optical and solid-state systems.

I. INTRODUCTION

Progress in engineering coherent quantum many-body systems with significant degree of the control makes it realistic to study properties of exotic quantum phases [1– 6] and to prototype quantum algorithms [7–10]. One of the key issue in the future scaling of such system is preserving their coherent properties when the system size is increased. Existing prototypes of quantum computing devices are based on various physical platforms, such as superconducting circuits [5], semiconductor quantum dots [11–13], trapped ions [3, 6, 9], neutral atoms [1, 2, 4], photons [14, 15], etc. The use of such objects as twolevel systems (qubits) in many cases is an idealisation since underlying physical systems are essentially multilevel. The idea of using additional levels of quantum objects for realizing quantum algorithms is at the heart of qudit-based quantum information processing. This approach has been widely studied last decades [16, 17], both theoretically and experimentally [18–55]. The most recent results is the pioneering realization of a universal multiqudit processors with trapped ions [56], superconducting [57] and optical systems [58].

Quantum algorithms within the digital quantum computing model can be presented as qubit-based circuits, so there are several approaches for processing them using qudits. First of all, qudits can be decomposed of a set of qubits [19–21, 35, 36]. This approach decreases the cost in realizing quantum algorithms by replacing some of two-qubit operations requiring interaction between distinct physical objects by single-qudit ones, which do not require such an interaction. However, this method is not universal in the sense that the total number of operations strongly depends on the mapping, i.e. the way of how qubits are encoded in qudits. As we demon-

strate below, specific mappings applied to specific qubit circuits may even lead to a substantial increase in the number of operations in comparison with the standard qubit-based approach. Second, higher qudit levels can be used for substituting ancilla qubits [30, 40, 59, 60]. This is especially important for decomposing multiqubit gates, such as the generalized Toffoli gate. In particular, an additional (third) energy level of the transmon qubit has been used in the experimental realization of Toffoli gate [46] (see also Refs. [61, 62]), which is a key primitive of many quantum algorithms, such as Shor's and Grovers's algorithms. While existing quantum computing schemes that are based on qubits platform benefit from a number of approaches for the realization of quantum algorithms, which requires compilers, transpilers, and optimizers, qudit-based quantum computing remains described mostly at the level of logic operations [63].

In the present work, we propose a technique for an efficient realization of qubit-based quantum algorithms, which employs the combination of two aforementioned approaches for the use of additional levels of gudits. The crucial element of our method is a transpilation of a qubit circuit, which depends on the parameters of an accessible qudit-based processor (e.g., number of levels and fidelity of operations). As a result, one obtains qubitto-qudit mapping and comparison to the standard qudit realization. A qudit circuit can be executed via quantum processors or classical emulators, and corresponding outcomes can be further post-processed in order to be interpreted as results of an algorithm. We develop an explicit scheme of transpiling qubit circuits into sequences of single-qudit and two-qudit gates taken from a particular universal set, which can be different for quantum processors based on various physical platforms. We provide an example of the gudit-based transpilation for the

case of a 6-qubit quantum algorithm.

The paper is organized as follows. In Sec. II, we revise the basic principles of quantum computing with qubits. In Sec. III, we discuss the general approach for implementing qubit circuit on qudit-based processors. In Sec. IV, we provide a concrete realization of a qudit-based transpiler. In Sec. V, we present an example of applying the developed approach for realizing 6-qubit circuits with four 4-level qudits. Finally, we conclude in Sec. VI.

II. QUBIT-BASED APPROACH

We start our consideration with a brief description of a standard quantum computation with qubits. The essence of qubit-based quantum computation is applying an unitary operator $U_{\rm circ}^{\rm qb}$ to a set of n two-level particles (qubtis), initialized in the fixed state $|0\rangle^{\otimes n}$, and the measuring the resulting state in the computational basis to obtain a sample from the following distribution:

$$p^{\rm qb}(x) = \left| \langle x | U_{\rm circ}^{\rm qb} | 0 \rangle^{\otimes n} \right|^2.$$
 (1)

Here we denote computational basis sates of qubits as $|0\rangle$ and $|1\rangle$, $|x\rangle \equiv |x_0\rangle \otimes \ldots \otimes |x_{n-1}\rangle$, and $x = (x_0, \ldots, x_{n-1}) \in \{0, 1\}^n$. Commonly, the same circuit is executed several times, which results in a sequence of independent and identically distributed (i.i.d.) random n-bit strings $(x^{(1)}, \ldots, x^{(N)})$, where N is a number of samples, and each sample $x^{(i)}$ is obtained from distribution (1).

The operator $U_{\rm circ}^{\rm qb}$ is originally represented in a form of a sequence of some standard unitary operators (gates) $U_i^{\rm qb}$ constituting hardware-agnostic (idealized) circuit circ $^{\rm qb}$. For applying $U_{\rm circ}^{\rm qb}$ to real physical particles, an additional transpilation step of decomposing $U_{\rm circ}^{\rm qb}$ to native (usually, single-qubit and two-qubit) operations is required [63–65]. One of the DiVincenzo's criteria [66] to quantum processors is the requirement to realize a universal set of gates that allows obtaining an efficient approximation of an arbitrary unitary operation up to a predefined accuracy. Although, multiqubit processors based on various physical principles have been demonstrated, the problem limited quality of quantum operations restricts computational capabilities of such systems. A particular issue is the realization of high-quality two-qubit quantum operations that require interactions between quantum information carriers.

III. QUANTUM COMPUTING WITH QUDITS

The idea of using of qudits, i.e. d-level quantum systems with d > 2, have been widely considered in the context of quantum information processing [18–55]. Clearly, an m-qudit system can be used for in order to obtain the same result as in the case of qubit-based computing –

Running qubit circuit with qudit-based processor (emulator)

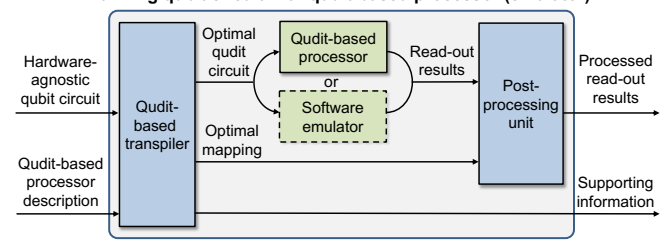


Figure 1. The main stages of implementing a qubit circuit with a qudit-based processor or emulator.

obtaining the number of samples coming from the distribution determined by an n-qubit circuit, but potentially with fewer resources, e.g. smaller number of information carriers and/or operations. The dimension of qudits and their number have to be compatible with the given n-qubit circuit. In what follows, we assume that $d^m \geq 2^n$.

A specific question that we are interested in is a transpilation of a circuit in the qubit form depending on the parameters of a qudit-based processor. A scheme of our approach is presented in Fig. 1. It consists of the three following stages: (i) qubit-to-qudit circuit transpilation, (ii) circuit execution, and (iii) classical post-processing of the measurement results. We note that stages (i) and (iii) are performed with a classical computer, while stage (ii) is realized with an accessible qudit-based processor or its classical software emulator.

The input for our scheme is a hardware-agnostic qubit circuit $\operatorname{circ}^{\operatorname{qb}}$, necessary runs number N, and the general information about the accessible qudit-based processor, specifically, the number of qudits m, their dimension d, and the set native gates (usually, it consists of single-qudit gates and a set of two-qudits gates within certain connectivity graph indicating on the possibility of direct realization of a two-qubit/two-qudit operation). The output of the transpilation step is an 'optimal' qudit circuit $\operatorname{circ}^{\operatorname{qd}}_{\operatorname{opt}}$, which is a sequence of native qudit gates, and an 'optimal qubit-to-qudit mapping' that is an injective function

$$\phi_{\text{opt}}: \{0,1\}^n \to \{0,1,\dots,d-1\}^m,$$
 (2)

assigning a qudit's computational basis state to each of qubits' ones. The general idea is that running of $\operatorname{circ}_{\operatorname{opt}}^{\operatorname{qd}}$ and processing the output measurement outcomes according to $\phi_{\operatorname{opt}}$ provides bitstrings equivalent to ones obtained after running $\operatorname{circ}^{\operatorname{qb}}$ on a standard qubit-based quantum processor (we formulate an rigorous consistency condition below). The term optimal appears here due to the fact that different qubit-to-qudit mappings, which are assignments between qubits' and qudits' levels, results in different qudit-based circuits that are equivalent to the input qubit-based circuit under particular mapping. In this way, the goal of the qudit-based transpiler is not only in transforming qubit gates of $\operatorname{circ}^{\operatorname{qb}}$ to native qudit ones, but also in finding a favorable mapping such that the realization of resulting qudit-based circuit is beneficial over

the straightforward realization of circ^{qb} on a qubit-based processor. Note that the optimal mapping depends both on the input circuit (it can be different for different circuits) and the architecture of the accessible qudit-based processor.

The optimality of mapping can be defined in different ways. Below we consider a particular implementation of a qudit-based transpiler, where we use a number of two-qudit gates as the main figure merit for quantifying the performance of the transpilation (see Sec. IV). The reason for this is that usually two-body gates is the main source of errors during the process of executing quantum circuits. Nevertheless, alternative metrics, such circuit depth or resulting fidelity estimation, can be used.

To achieve the goal of reducing the number of twobody gates in going from qubits to qudits, two main techniques, as well as their combination, can be implemented. The first technique [19–21, 35, 36], employs a qudit's d-dimensional space for embedding several qubits (the technique works for $d \geq 2^{m'}$ with m' > 1). The main advantage of this technique is the possibility to reduce the number of employed physical information carriers (e.g., particles, such as atoms or ions). However (as we show in Sec. IV), this method is not universal in the sense that the total number of operations strongly depends on the mapping, i.e. the way of how gubits are embedded in qudits. It appears that the cost of the realization of two-qubit operations between two qubits inside one qudit may be close to a couple of singe-qubit operations, since it does not require any interaction between distinct physical particles. In contrast, the realization of a two-qubit operation between qubits belonging to different qudits, additional entangling operations are required in order to presume the state of other qubits inside these qudits but untouched by the two-qubit gate.

The second technique is to use 'upper' qudit levels ($|a\rangle$, $a \geq 2$) for substituting ancillary qubits within standard multiqubit gates decompositions [30, 40, 45, 59, 60]. This approach allows decreasing both the number of required two-body interactions and number of employed quantum information carriers by removing necessity of ancillary qubits and useful in the case of quantum circuits containing multiqubit gates. We would like to note that these two approaches can be combined in the case of $d > 2^t$ for some $t \geq 2$: The first t levels of a qudit can be used for embedding $\lfloor \log_2 t \rfloor$ qubits, while the remaining ones can be used for subsisting ancillas.

There are two aspects regarding the qudit-based transpilation. The first point is related to the possibility of realizing qudit gates. As for qubits, a universal set of gates can be composed of arbitrary single-qudit gates, supplemented with one two-qudit entangling gate. One of the approaches for designing this two-qudit gate is to employ an original two-qubit gate, yet considered in the extended qudit state space. Such as approach have been demonstrated in experiments with trapped ions [56]. We note that fidelities are comparable with the experiments on qubit systems and can be further improved [56].

The second point is about finding the best possible mapping among possible. In the case of small- and intermediate-scale circuits one may use exhaustive search through all possible mappings. This is the approach we use in our gudit-based transpiler. However, this approach is not scalable and directly applicable for large-scale circuits. In this case, one is suffice to find a mapping that eventually is not the best-possible one, but still gives the number of two-body gates that is lower than in the standard qubit implementation (or gives a higher fidelity). The development of polynomial time approximate optimization algorithms for this problem is an interesting problem requiring a separate research. Indeed, if the number of available qudits m is not less than the number of qubits in the input circuit n, then there is a trivial mapping, where each qubit is embedded in its own qudit. In this case, the number of two-body gates in implementing qubit circuit with qudits can not be less than the number of two-body gates of the standard qubit-based realization of the circuit on the same processor. The comparison between the number of two-body gates for the best found mapping with the number of two-body gates for the straightforward qubit-based implementation can serve as a benchmark for the efficiency of the gudit-based transpilation process (see Fig. 1).

When an exhaustive search is not applicable, the problem of finding approximate solution can be tackled by using the following observations. First, it is advisable to consider embedding a pair of two qubits into the space of a single qudit, if the there is a relatively huge amount of two-qubit gates connecting these qubits within the given circuit, and there is relatively small amount of gates affecting each of this qubits separately. Second, it is resonable to put qubits affected by multiqubit gates into audits with free upper levels to use these levels as ancillas for multiqubit gates decomposition. We note that in the qutrit case (d=3) and $m \geq n$, there is no need in searching for optimal mapping: One can employ nqutrits, each used as a qubit plus the ancillary state. In this case, all single-qubit and two-qubit gates of the original circuit are transpiled as usual (the third qutrit level remains not occupied), while multiqubit gates are decomposed using techniques from [40, 59, 60]. We also note that if a gudit-based transpilation rule for each possible gate in a hardware-agnostic circuit is known, as it is the case for our transpiler, then the (classical) computation time for transpilation with respect particular mapping is obtained with time scaling linearly with the number of gates in the original circuit. We discuss all the technical details of a particular realization of qudit-based transpilation in the next section.

Let us back to the description of main stages of running the qubit-based circuit with the qudit-based processor shown in Fig. 1. At stage (ii), the qudit circuit $\operatorname{circ}_{\operatorname{opt}}^{\operatorname{qd}}$ is the input for the qudit-based processor (or emulator) that applies the gates from $\operatorname{circ}_{\operatorname{opt}}^{\operatorname{qd}}$ to the qudit register initialized in the state $|0\rangle^{\otimes m}$, where we use $\{|l\rangle\}_{l=0}^{d-1}$ to denote computational basis states of each qudit. The

resulting qudit state is measured in the computational basis, and a sample from the following distribution is obtained:

$$p^{\mathrm{qd}}(y) = \left| \langle y | U_{\mathrm{circ}}^{\mathrm{qd}} | 0 \rangle^{\otimes m} \right|^2, \tag{3}$$

where $U_{\mathrm{circ}}^{\mathrm{qd}}$ is the resulting qudit unitary operator, $y = (y_0, \ldots, y_{m-1}), y_i \in \{0, \ldots, d-1\}$, and $|y\rangle \equiv |y_0\rangle \otimes \ldots \otimes |y_{m-1}\rangle$. The circuit is run N times, that yields a N-length sequence $(y^{(1)}, \ldots, y^{(N)})$, where each $y^{(i)}$ is the string of m numbers from $\{0, \ldots, d-1\}$.

The final post-processing stage takes the read-out results $(y^{(1)}, \ldots, y^{(N)})$ and a mapping ϕ in order to obtain equivalent qubit outcomes $(\phi^{-1}(y^{(1)}), \ldots, \phi^{-1}(y^{(N)}))$ as input, where ϕ^{-1} outputs n-length bit strings out of $y^{(i)}$. The general condition for the scheme correctness is as follows:

$$p^{\mathrm{qd}}(y) = p^{\mathrm{qb}}(\phi^{-1}(y)), \quad y \in \mathrm{image}(\phi),$$
 (4)

where $\operatorname{image}(\phi)$ is the set of all possible outputs of the mapping ϕ . The consistency condition (4) guarantees that only $y \in \operatorname{image}(\phi)$ can appear as measurements results of the qudit-circuit, and the obtained bit strings $(\phi^{-1}(y^{(1)}),\ldots,\phi^{-1}(y^{(N)}))$ are indistinguishable from ones that can be obtained with a qubit-based processor. The set of bitstrings $(\phi^{-1}(y^{(1)}),\ldots,\phi^{-1}(y^{(N)}))$ together with the supporting information is the final output of our approach. One can see that from the viewpoint of classical processing, the most challenging is the qudit-based transpilation stage. We discuss it in the detail below.

IV. QUDIT-BASED TRANSPILATION

Here we describe the concrete realization of the quditbased transpiler designed for a specific model of a quditbased processor. We assume that the available processor consists of m d-dimensional qudits, labeled as $Q1, \ldots, Qm$. We also assume that m and d are reasonably small that is important for finding the optimal mapping (we discuss this issue in Sec. IV A). However, we note the general gate transpilation (this is discussed in Sec. IV B), scheme works with arbitary m and d. As a set of native qudit gates, we consider single qudit operations

$$R_{\mathbf{Q}j}^{\alpha,\beta}(\varphi,\theta) = \exp(-i\theta\sigma_{\varphi}^{\alpha,\beta}/2),$$

$$Ph_{\mathbf{Q}j}^{\alpha}(\theta) = \operatorname{diag}(1,\dots,1,e^{i\theta},1,\dots,1),$$
(5)

where $e^{\imath\theta}$ is located in α th position, and a two-qudit operation

$$CZ_{Qj_1,Qj_2}^{\alpha,\beta} = \mathbb{1}_{Qj_1} \otimes \mathbb{1}_{Qj_2} - 2 |\alpha\beta\rangle_{Qj_1,Qj_2} \langle \alpha\beta|.$$
 (6)

Here we use the following notations:

$$\sigma_{\phi}^{\alpha,\beta} = \sigma_{x}^{\alpha,\beta} \cos \varphi + \sigma_{y}^{\alpha,\beta} \sin \varphi,$$

$$\sigma_{\xi}^{\alpha,\beta} = \langle 0 | \sigma_{\xi} | 0 \rangle | \alpha \rangle \langle \alpha | + \langle 0 | \sigma_{\xi} | 1 \rangle | \alpha \rangle \langle \beta | +$$

$$\langle 1 | \sigma_{\xi} | 0 \rangle | \beta \rangle \langle \alpha | + \langle 1 | \sigma_{\xi} | 1 \rangle | \beta \rangle \langle \beta |, \ \xi \in \{x, y, z\},$$

$$(7)$$

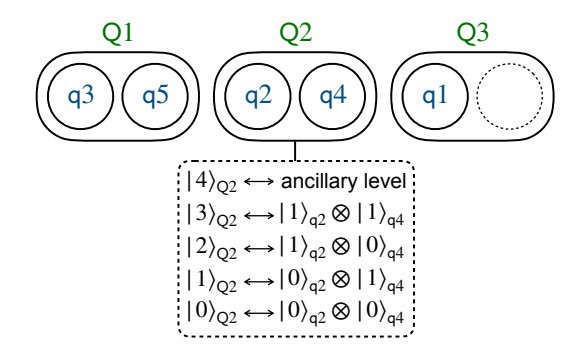


Figure 2. Example of a mapping in the form, given by (10) and (11), between n=5 qubits and m=3 qudits of dimension d=5. Within the presented mapping, position_in_qudit[q4] = 2, qudit_index[q4] = Q2, and qubit_index[Q2, 2] = q4.

 σ_x , σ_y , σ_z are standard single-qubit Pauli matrices, $\alpha, \beta \in \{0, \dots, d-1\}$ denote levels in qudits' space, φ, θ are real-valued arbitrary angles, and $\mathbbm{1}$ stands for the identity matrix. In what follows we use subindices over unitary operators in order to specify quantum information carrier or carriers (qubits or qudits) at which this operator acts on. We assume that two-qudit gates can be implemented for every pair of qudits within all-to-all coupling map.

The input for the designed transpiler n-qubit hardware-agnostic qubit circuit $\mathsf{circ}^{\mathsf{qb}}$, acting of qubits denoted by $\mathsf{q1},\ldots,\mathsf{q}n$, is assumed to consist of single qubit gates

$$r_{\rm gi}(\varphi,\theta) = \exp(-i\theta\sigma_{\varphi}/2),$$
 (8)

where $\sigma_{\varphi} = \sigma_x \cos \varphi + \sigma_y \sin \varphi$, and a κ -qubit gates

$$CZ_{qi_1,...,qi_{\kappa}} = \mathbb{1}_{qi_1} \otimes \cdots \otimes \mathbb{1}_{qi_{\kappa}} - 2|1\dots1\rangle_{qi_1,...,qi_{\kappa}} \langle 1\dots1| \quad (9)$$

with $\kappa \in \{2, 3, \dots, n\}$. One can see that multi-body operations (6) and (9) correspond to acquiring a phase factor of -1 on a particular multi-body state. We note that a multi-qubit operation (6) can be transformed to a generalized Toffoli gate by applying single-qubit gates. We also note that both the considered qudit-based and qubit-based sets of gates are universal.

Without loss of generality, we assume that $\operatorname{circ}^{\operatorname{qb}}$ terminates with read-out measurements in a computational basis acting on each of n qubits. The initial state of qubit register is assumed to be $|0\rangle^{\otimes n}$.

For possible mappings between qubits' and qudits' spaces, we restrict ourselves with ones embedding the whole computational space of one or several qubits into a space of particular qudit. Specifically, each possible mapping ϕ can be defined in the following form:

$$\phi = (\phi_{Q1}, \dots, \phi_{Qm}), \quad \phi_{Qj} = (qi_{j,1}, \dots, qi_{j,\#j}), \quad (10)$$

meaning that qudit Qj contains #j qubits $\mathsf{q}i_{j,1},\ldots,\mathsf{q}i_{j,\#j}$ (given that the condition $2^{\#j} \leq d$

is fulfilled). The assignment of computational basis states of qubits to computational basis states of qudits is governed by corresponding binary representation:

$$|\operatorname{int}(x_1,\ldots,x_{\#j})\rangle_{\mathbf{Q}j} \leftrightarrow |x_1\rangle_{\mathbf{q}i_{j,1}} \otimes \ldots \otimes |x_{\#j}\rangle_{\mathbf{q}i_{j,\#j}}, (11)$$

where $x_1, \ldots, x_{\#j} \in \{0,1\}$ are bit values and $\operatorname{int}(x_1, \ldots, x_{\#j}) \in \{0,1,\ldots,2^{\#j}-1\}$ outputs an integer number from its binary representation $x_1,\ldots,x_{\#j}$. We note that within the considered mappings, the 'address' of each qubit is defined by an index of qudit $Qj \in \{Q1,\ldots,Qm\}$ and a 'position' $\operatorname{pos} \in \{1,\ldots,\#j\}$ of the qubit inside the qudit. An example of a possible mapping between n=5 qubits and m=3 qudits of the dimension d=5 is shown in Fig. 2.

To simplify operations within the considered special case of mapping ϕ , it is convenient to introduce the following functions:

$$\begin{split} & \mathsf{position_in_qudit}[\mathsf{q}i] \mapsto \mathsf{pos}, \\ & \mathsf{qudit_index}[\mathsf{q}i] \mapsto \mathsf{Q}j, \\ & \mathsf{qubit_index}[\mathsf{Q}j,\mathsf{pos}] \mapsto \mathsf{q}i, \end{split} \tag{12}$$

where the first two functions provide the address of a given qubit with the qudits' space, the the third function returns an index of a qubit given its address. We also introduce functions

indices_of_qubits[Q
$$j$$
] \rightarrow {q $i_{j,1}, \dots, qi_{j,\#j}$ }, number_of_qubits[Q j] \rightarrow # j (13)

that return indices of qubits located in a given qudit and the total number of qubits in a given qudit correspondingly.

The considered 'qubit-to-qudit' mapping, in particular Eq. (10), implies that the computational basis measurement in the end of qubit circuit corresponds to a computational basis measurement of qudits, also assumed to be realizable on the qudit-based processor.

The developed qudit transpiler consists of two modules: (i) the optimal mapping finder and (ii) the qudit circuit constructor (see Fig. 3). Both of them takes as input a qudit processor description (values of m and d) and a hardware-agnostic qubit-based circuit circ qb . The goal of the optimal mapping finder is to obtain the best possible mapping $\phi_{\text{opt}} \in \{\phi\}$, while the purpose of the qudit circuit constructor is to generate a qudit circuit circ $^{qd}_{\phi}$ that is equivalent to circ $^{qb}_{\phi}$ under a mapping ϕ . Finally, the qudit transpiler outputs the optimal mapping ϕ_{opt} and the corresponding circuit circ $^{qd}_{\phi_{\text{opt}}}$. Below we describe operation of modules in more details.

A. Optimal mapping finder

Within our realization of qudit-based traspiler, we consider a straightforward exhaustive search approach for finding the optimal mapping ϕ_{opt} over all possible mappings $\Phi \equiv \{\phi\}$ of the form Eq. (10). This is the reason

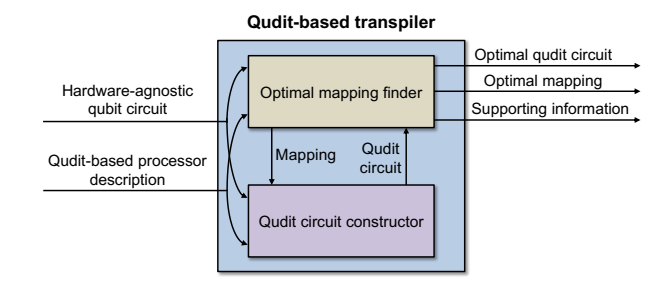


Figure 3. Data transfer scheme in the developed qudit-based transpiler.

why we assume that the number of available qudits m and their dimension d are reasonably small.

The optimal mapping finder works as follows. First, we construct a set of all non-equivalent mappings $\widetilde{\Phi} \subset \Phi$, where we call two mappings $\phi^{(1)}, \phi^{(2)} \in \Phi$ equivalent, if they are different only up to permutations of qubits indices within particular qudit, or up to permutation of whole sets of qubits' indices belonging to different qudits.

We note that in the special case of qutrits (d = 3), there is only one non-equivalent mapping: each qubit qi is mapped to a qudit Qi.

In Fig. 4 we show the behaviour of the total number of non-equivalent mappings $|\widetilde{\Phi}|$ for different values of n and d. We note that in Fig. 4 we take the number qudits m to be equal to the number of qubits n, to maximize the number of possible mappings. Since we deal with a special case of mappings, where each qubit is entirely embedded in a single qudit, the number of mappings for different qudit dimensions taken from a range $d = 2^{n'}, \ldots, 2^{n'} - 1$ for some n' is the same.

Then, the mapping finder consistently sends each $\phi \in \widetilde{\Phi}$ to the qudit circuit constructor that outputs the corresponding qudit circuit $\operatorname{circ}_{\phi}^{\operatorname{qd}}$. As we show below, the complexity of generating $\operatorname{circ}_{\phi}^{\operatorname{qd}}$ is linear with respect to the number of gates in the original qubit-based circuit $\operatorname{circ}^{\operatorname{qb}}$. Given the fact for $d \leq 31$ and $n \leq 7$, the resulting number of non-equivalent mappings is no more than thousand (see Fig. 4), it is possible to go through all $\phi \in \widetilde{\Phi}$ within a reasonable time.

As a main figure of merit of a mapping ϕ , we employ the number of two-qudit gates in $\mathsf{circ}_{\phi}^{\mathrm{qd}}$. The reason for this is that usually, it is two-qudit gates that are the main source of fidelity decreasing.

By consistent pair-wise comparison of two-qudit gate numbers in $\operatorname{circ}_{\phi}^{\operatorname{qd}}$ while going through all $\phi \in \widetilde{\Phi}$, we find the one $(\phi_{\operatorname{opt}})$ that provides the smallest number of two-qudit gates. We note that no more than two qudit-based circuits have to be stored in a memory of a classical computer during the search process.

As we have mentioned before, alternatively one can employ other figures of merits, e.g. circuit depth or fidelity estimations that also can be efficiently calculated given classical representation of corresponding qudit-

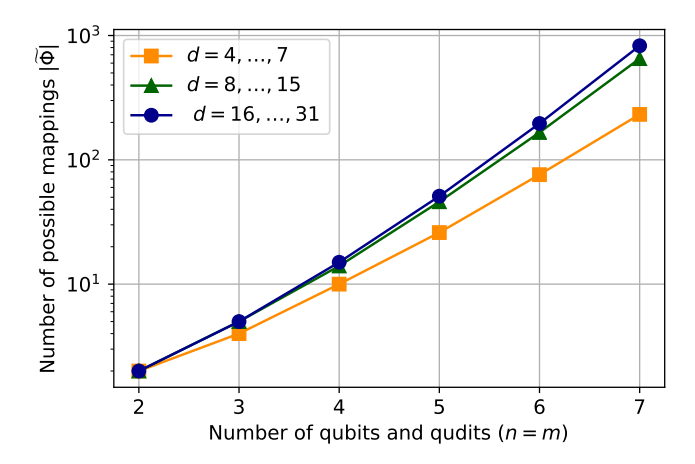


Figure 4. The total number of non-equivalent mapping $|\tilde{\Phi}|$ depending on the number of qudits m for $d \in \{4, \ldots, 31\}$. To maximize the number of nonequivalent mappings, we take the number of qubits n the same as the number of qudits m.

based circuit.

As an additional feature, the optimal mapping finder can perform a comparison of circ^{qb} and circ^{qd}_ϕ , providing supporting information for the final output. For example, supporting information may contain exact number of single-qudit and two-qudit gates in $\mathsf{circ}^{qd}_{\mathrm{opt}}$ and its comparison with the number of single- and two-qubit gates in $\mathsf{circ}^{qb}_{\mathrm{using}}$ the usual qubit-based gates decomposition (transpilation). Below we consider in detail how qudit circuit constructor transpiles qubit circuit $\mathsf{circ}^{qb}_{\phi}$ to the qudit circuit $\mathsf{circ}^{qd}_{\phi}$ according to the given 'qubit-to-qudit' mapping ϕ .

B. Qudit circuit constructor

The traspilation process of $\operatorname{circ}^{\operatorname{qb}}$ into $\operatorname{circ}^{\operatorname{qd}}_{\phi}$ is performed in a gate-by-gate principle shown in Fig. 5. At very beginning of the process, $\operatorname{circ}^{\operatorname{qd}}_{\phi}$ is initialized as empty. Then, for each gate from the qubit circuit $\operatorname{circ}^{\operatorname{qb}}$, the constructor takes a set

$$qubit_set = \{qi_1, \dots, qi_{\kappa}\}. \tag{14}$$

of qubits, affected by this gate, and finds the set of corresponding qudits, possessing qubits from qubit_set:

$$qudit_set = \{qudit_index[qi_1], \dots, qudit_index[qi_{\kappa}]\}.$$
 (15)

We note that $qudit_set$ does not contain duplicates of qudit indices. So, the number of elements in $qudit_set$, which we denote by $|qudit_set|$, can be less than the number of involved qubits κ if several affected qubits are located in the space of the same qudit according to the mapping ϕ .

The processing of the gate is determined by the value of |qudit_set|. If |qudit_set| = 1, then the qubit gate under processing can be realized on the qudit processor as

a sequence of single-qudit gates (see subsection IVB1). In the case of |qudit_set| > 1, two-qudit gates become necessary. It is convenient to distinguish the case of |qudit_set| = 2 and the case of |qudit_set| ≥ 3 that we describe in details in sections IVB2 and IVB3, correspondingly. For all these cases we obtain a sequence of qudit gates that implement the processed qubit gate. This sequence is added to the end of $\mathrm{circ}_\phi^{\mathrm{qd}}$, and then the procedure is repeated for the next gate from $\mathrm{circ}^{\mathrm{qb}}$ until all until all gates have been processed. Below we describe exact decomposition of qubit gates into the sequence of qudit gates for all possible values of |qudit_set|.

1. Single-qudit case

The case of |qudit_set| = 1 can appear in two situations: (i) the processed gate is a single-qubit one ($\kappa = 1$), and (ii) the processed gate in a multi-qubit ($\kappa \geq 2$) with all affected qubits being located in the same qudit according to the mapping ϕ .

First, let us consider the case of a single-qubit gate, acting on a qubit qi_1 . Let $Qj = \text{qudit}_{index}[qi_1]$, pos = position_in_qudit[qi_1], and $\#j = \text{number}_{of}_{qubits}[Qj]$. Remind that in our realization, the only type of single-qubit gates is rotation $r_{qi}(\varphi,\theta)$, defined in Eq. (8). To implement this unitary in the qudit's space, we need to consider a tensor product of a 2 × 2 unitary acting in a subspace of affected qubit with an identity operation acting in the remaining space of a qudit. The resulting correspondence between the qubit gate and a sequence of qudit gates is given by

$$r_{qi}(\varphi,\theta) \to \prod_{(\alpha,\beta)} R_{Qi}^{\alpha,\beta}(\varphi,\theta),$$
 (16)

where the product is made over all possible pair levels (α, β) satisfying the following condition:

$$bin(\alpha) = x_1 \dots x_{pos-1} 0 \ x_{pos+1} \dots x_{\#j},$$

$$bin(\beta) = x_1 \dots x_{pos-1} 1 \ x_{pos+1} \dots x_{\#j}.$$
(17)

Here $\operatorname{bin}(\alpha)$ and $\operatorname{bin}(\beta)$ are #j-length binary representation of α and β , correspondingly (let us remind that $\alpha, \beta \in \{0, 1, \dots, d-1 \text{ and } \#j \leq \log_2 d\}$, and $x_1 \dots x_{\mathsf{pos}-1} x_{\mathsf{pos}+1} \dots x_{\#j}$ are all possible bitstrings of length #j-1. The sequence of qudit unitaries, given by Eqs. (16) and (17), is in agreement with employed structure of 'qubit-to-qudit' mappings shown in Eq. (11) [see also Fig. 6(a) for an intuitive explanation].

Let us then consider the case of a multi-qubit gate $\mathsf{CZ}_{\mathsf{q}i_1,\ldots,\mathsf{q}i_\kappa}$, where all qubits $\mathsf{q}i_1,\ldots,\mathsf{q}i_\kappa$ are located in the same qudit $\mathsf{Q}j$. Let $\mathsf{pos}_{i_k} = \mathsf{position_in_qudit}[\mathsf{q}i_k]$ for $k=1,\ldots,\kappa$. Then the desired gate $\mathsf{CZ}_{\mathsf{q}i_1,\ldots,\mathsf{q}i_\kappa}$ can be realized with the following sequence of single-qudit phase gates:

$$\mathsf{CZ}_{\mathsf{q}i_1,\ldots,\mathsf{q}i_\kappa} \to \prod_{\alpha} \mathsf{Ph}_{\mathsf{Q}j}^{\alpha}(\pi),$$
 (18)

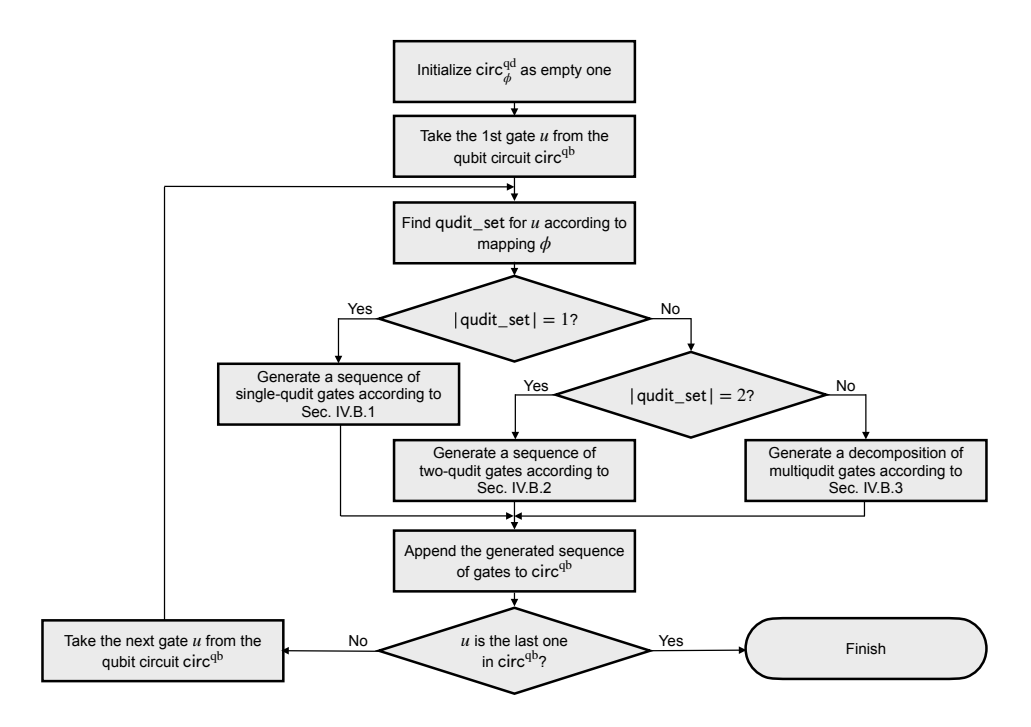


Figure 5. Qudit circuit transpilation algorithm implemented in the qudit-based circuit constructor. Gates from circ^{qb} are sequentially classified by a number of qudits in qudit_set and then transpiled to qudit-based gates depending on the number of qudits in qudit_set.

where qudit levels α satisfy the following condition:

$$bin(\alpha)[pos_{i_k}] = 1 \text{ for each } k = 1, \dots, \kappa$$
 (19)

(here $bin(\alpha)[pos_{i_k}]$ stands for pos_{i_k} th bit in a #j-length binary representation of α). As in the case of single-qubit gate, the resulting sequence provides a proper transformation at required qudit levels [see Fig. 6(b)].

$$2. \quad Two-qudit\ case$$

Here we consider the case where qubits, which are involved in certain multi-qubit gate $\mathsf{CZ}_{\mathsf{q}i_1,\ldots,\mathsf{q}i_\kappa}$, are located (according to ϕ) in two different qudits, namely $\mathsf{Q}j_1$ and $\mathsf{Q}j_2$. Let $\{\mathsf{pos}_1^l\}$ and $\{\mathsf{pos}_2^{l'}\}$ be positions, according to $\mathsf{position_in_qudit}[\cdot]$, of qubits located at $\mathsf{Q}j_1$ and $\mathsf{Q}j_2$, correspondingly.

As in the case of a single-qubit gate, the resulting transformation performed in the space of two qudits is obtained as a tensor product of the unitary corresponding to $\mathsf{CZ}_{\mathsf{q}i_1,\ldots,\mathsf{q}i_\kappa}$ in the proper subspace of two-qudits' space and identity operator in the remaining subspace. This operation reads

$$CZ_{qi_1,\dots,qi_{\kappa}} \to \prod_{(\alpha,\beta)} CZ_{Qj_1,Qj_2}^{\alpha,\beta}, \tag{20}$$

where pairs of levels (α, β) are all possible admissible pairs satisfying the condition

$$\operatorname{bin}(\alpha)[\operatorname{pos}_1^{\ell}] = 1, \quad \operatorname{bin}(\beta)[\operatorname{pos}_2^{\ell'}] = 1. \tag{21}$$

According to Eqs. (20) and (21), the number of $\mathsf{CZ}_{\mathsf{Q}j_1,\mathsf{Q}j_2}^{\alpha,\beta}$ gates in the resulting sequence is determined by the number of qubits located in qudits $\mathsf{Q}j_1$ and $\mathsf{Q}j_2$ and not involved by $\mathsf{CZ}_{\mathsf{q}i_1,\ldots,\mathsf{q}i_\kappa}$ (see an example for two-qudit case in Fig. 7). Each unused qubit doubles the number of pairs (α,β) satisfying Eq. (21), and so the resulting number of two-qudit gates is given by

$$2^{\#j_1 + \#j_2 - \kappa},\tag{22}$$

where $\#j_1$ and $\#j_2$ are number of qubits in $\mathbb{Q}j_1$ and $\mathbb{Q}j_2$ correspondingly.

One can see that Eq. (22) manifests itself in two ways. One the one hand, implementation of, let say, two-qubit gates ($\kappa = 2$) in the case where qudits Qj_1 and Qj_2 contain other qubits $(\#j_1 + \#j_2 > 2)$ costs more twobody interactions than in the case of direct qubit-based realization $(2^{\#j_1+\#j_2-1}$ compared to 1). On the other hand, in the case of multi-qubit gates with $\kappa > 2$, the resulting number of two-body interactions can become smaller compared to the one obtained from known multiqubit gates decompositions into single-qubit and twoqubit gates (see e.g. Ref. [67]). We also remind that in the case where all qubits affected by $\mathsf{CZ}_{\mathsf{q}i_1,\dots,\mathsf{q}i_\kappa}$ fall into the same qudit, there is no need in two-body interactions at all. This is how the mapping plays a critical role for the number of two-qudit gates and resulting fidelity of circuit implementation.

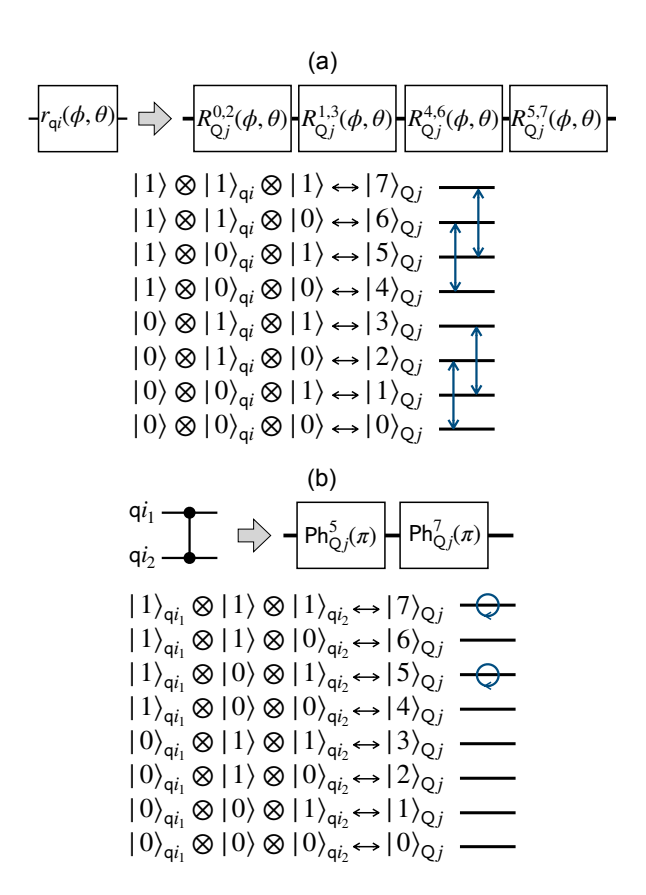


Figure 6. (a) Qudit-based realization of a single-qubit gate $r_{\mathbf{q}i}(\varphi,\theta)$ in the case where $\mathbf{q}i$ is embedded into 8-level qudit $\mathbf{Q}j$ at the 2nd position ($\mathbf{Q}j$ contains three qubits in total). The involved transitions within the 8-level qudit $\mathbf{Q}j$ are shown. (b) Qudit-based realization of a two-qubit gate $\mathsf{CZ}_{\mathsf{q}i_1,\mathsf{q}i_2}$ in the case where the affected qubits $\mathsf{q}i_1$ and $\mathsf{q}i_2$ are embedded into the same qudit $\mathsf{Q}j$ at the 1st and 3rd positions, correspondingly. The levels acquiring the phase factor of -1 are shown.

3. Multi-qudit gate case

Here we describe the most complicated case, where qubits affected by the gate $\mathsf{CZ}_{\mathfrak{q}i_1,\ldots,\mathfrak{q}i_\kappa}$, fall into more than two qudits. To make decomposition description more clear, let us introduce new notations. For each qudit Qj, we define states $|\underline{0}\rangle_{Qj} \equiv |0\rangle_{Qj}$ and $|\underline{1}\rangle_{Qj} \equiv |d^2-1\rangle_{Qj}$ that corresponds to multi-qubit states $|0\ldots 0\rangle_{\mathfrak{q}i_j,1,\ldots,\mathfrak{q}i_j,\#_j}$ and $|1\ldots 1\rangle_{\mathfrak{q}i_{j,1},\ldots,\mathfrak{q}i_{j,\#_j}}$, correspondingly, with respect to the considered mapping ϕ (remind that $\mathfrak{q}i_{j,1},\ldots,\mathfrak{q}i_{j,\#_j}$ denote labels of qubits located in the space of qudit Qj). If qudit dimension $d>2^{\#j}$, we also define an ancillary state $|a\rangle_{Qj}\equiv|2^{\#j}\rangle_{Qj}$ that is beyond the qubits' subspace in the space of Qj, and a flag, indicating whether the ancillary level is available in this qudit:

$$\operatorname{ancilla}[\mathsf{Q}j] = \begin{cases} \mathsf{True}, & \text{if } d \ge 2^{\#j}, \\ \mathsf{False}, & \text{otherwise.} \end{cases} \tag{23}$$

Let qudit_set be a set of qudit indices involved in the

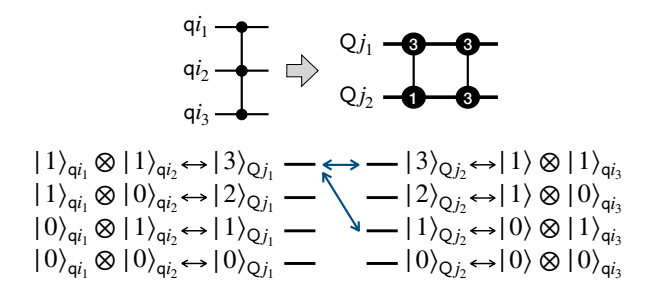


Figure 7. Qudit-based realization of a three-qubit gate $\mathsf{CZ}_{\mathsf{q}i_1,\mathsf{q}i_2,\mathsf{q}i_3}$ in the case where $\mathsf{q}i_1$ and $\mathsf{q}i_2$ are embedded into $\mathsf{Q}j_1$ and $\mathsf{q}i_3$ together with some other qubit are embedded into $\mathsf{Q}j_2$ correspondingly $(\mathsf{Q}j_1 \text{ and } \mathsf{Q}j_2 \text{ are 4-level systems})$.

realization of $\mathsf{CZ}_{\mathsf{q}i_1,\ldots,\mathsf{q}i_\kappa}$, see Eq. (15). We assign each qudit from qudit_set to one of three possible types labeled as \mathcal{A} , \mathcal{B} , or \mathcal{C} .

We say that Qj belongs to type \mathcal{A} , if all qubits, located in this qudit, are affected by $\mathsf{CZ}_{\mathsf{q}i_1,\ldots,\mathsf{q}i_\kappa}$ and Qj has no ancillary level, that is

$$(indices_of_qubits(Qj) \subset qubit_set) \land \overline{ancilla[Qj]}, (24)$$

where $\operatorname{ancilla}[Qj]$ stands for $\operatorname{ancilla}[Qj] = \operatorname{False}$. If all qubits located in qudit Qj are involved in the decomposed qubit gate and Qj has ancillary level, that is

$$(indices_of_qubits[Qi] \subset qubit_set) \land ancilla[Qi], (25)$$

then we say that qudit Qj belongs to type \mathcal{B} . Qudit $Qj \in \text{qudit_set}$ belongs to type \mathcal{C} if there is at least one qubit located in Qj but not affected by $\mathsf{CZ}_{\mathsf{q}i_1,\ldots,\mathsf{q}i_\kappa}$:

$$(Qj \in qudit_set) \land (indices_of_qubits[Qj]/qubit_set \neq \varnothing).$$
(26)

We denote the number of qudits of types \mathcal{A} , \mathcal{B} , and \mathcal{C} as $|\mathcal{A}|$, $|\mathcal{B}|$, and $|\mathcal{C}|$, correspondingly.

The transpilation of $\mathsf{CZ}_{\mathsf{q}i_1,\dots,\mathsf{q}i_\kappa}$ is performed by, first, constructing an intermediate qudit circuit $\mathsf{circ}_\phi^{\mathsf{qd-int}}$ presented in Fig. 8(a), and then decomposing $\mathsf{circ}_\phi^{\mathsf{qd-int}}$ down to single-qudit and two-qudit gates.

We then split $\operatorname{circ}_{\phi}^{\operatorname{qd-int}}$ into five steps: (i) multi-qudit controlled gate with controls on type \mathcal{A} qudits and target on the first qudit of type \mathcal{B} ; (ii) down step ladder-like sequence of two-qudit gates on all qudits of type \mathcal{B} ; (iii) multi-qudit gate acting on the last qudit of type \mathcal{B} and all qudits of type \mathcal{C} ; (iv) up step ladder-like sequence that is uncomputation of step (ii); (v) uncomputation of step (i).

The general idea of this structure is as follows. According to $\mathsf{CZ}_{\mathsf{q}i_1,\ldots,\mathsf{q}i_\kappa}$, we have to add an additional phase factor -1 to all basis states of involved qudits such that all corresponding qubits $\mathsf{q}i_1,\ldots,\mathsf{q}i_\kappa$, embedded in these qudits, are in the state 1. We note that for qudits of types \mathcal{A} and \mathcal{B} , there is a single level that is a candidate for acquiring the phase factor, namely $|\underline{1}\rangle$. For type \mathcal{C} qudits, the situation is different. Since the presence of

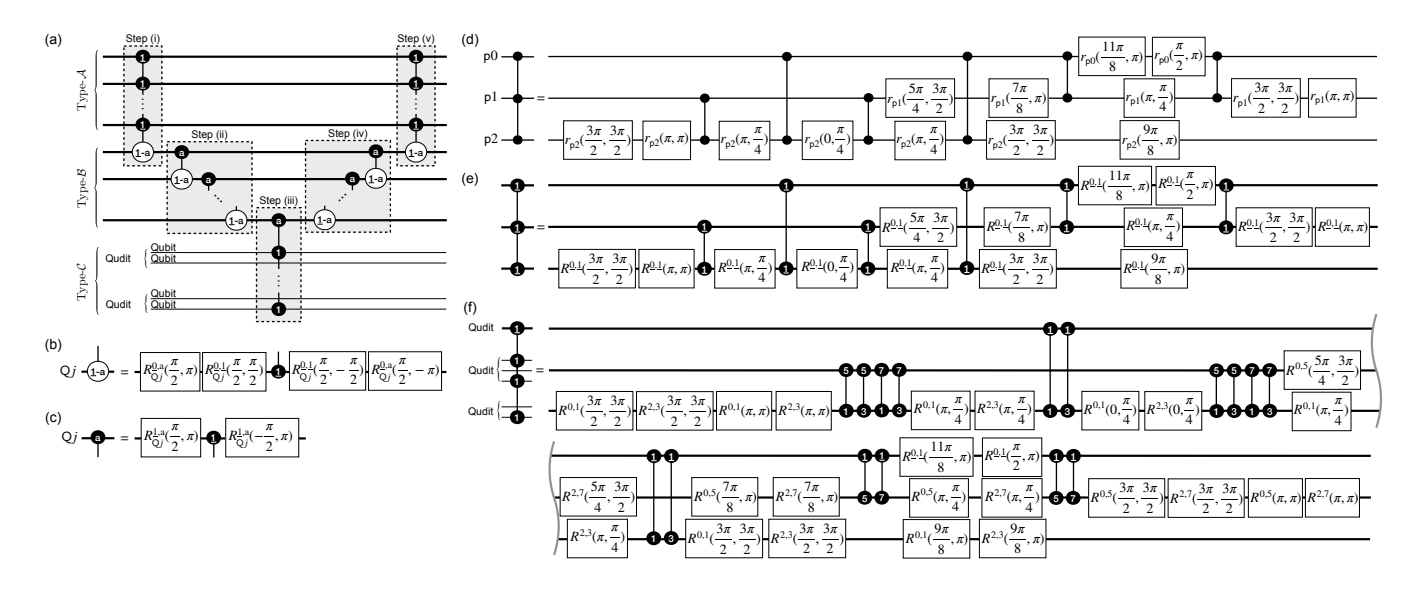


Figure 8. (a) Intermediate qudit circuit $\operatorname{circ}_{\phi}^{\operatorname{qd-int}}$ used for the decomposition of $\operatorname{CZ}_{\mathfrak{q}i_1,\ldots,\mathfrak{q}i_\kappa}$ with $|\operatorname{qudit_set}| \geq 3$. Each gate of $\operatorname{circ}_{\phi}^{\operatorname{qd-int}}$ is then transpiled down to native single-qudit and two-qudit gates. (b) The scheme of transforming an inversion operation between levels $|\underline{1}\rangle$ and $|a\rangle$ to the phase accruing operation at level $|\underline{1}\rangle$ via single-qudit operations. (c) The scheme of transforming a control at level $|a\rangle$ to the control at level $|\underline{1}\rangle$ via single-qudit operations. (d) An example of the qubit-based ancilla-free decomposition of three-qudit $\operatorname{CZ}_{p0,p1,p2}$ gate according Ref. [67] that can be used as a template to decompose multiqudit CZ type gates at Steps (i), (iii), and (v). (e) Decomposition of a three-qudit gate used in Steps (i) and (v) to single-qudit and two-qudit gates according to the template, shown in (d). (f) Decomposition of a three-qudit gate used in Step (iii) to single-qudit and two-qudit gates according to the template, shown in (d).

unaffected qubits, the phase factor is acquired or not acquired (depending on the state of other involved qudits), to several levels of type $\mathcal C$ qudit, namely to all levels α satisfying the condition

$$bin(\alpha)[pos] = 1, \tag{27}$$

where pos values corresponds to positions of affected qubits in the considered qudit. Roughly speaking, we need to add a phase factor of -1 to a computational basis state of involved qudits, if all type- $\mathcal A$ and type- $\mathcal B$ qudits are in the state $|\underline{1}\rangle$, and all qubits encoded in type- $\mathcal C$ qudits are in the state $|1\rangle$.

The important feature of type \mathcal{B} -qudits is that they posses an ancillary level that can be employed for storing temporary information within the gate decomposition. We use an ancillary level of type \mathcal{B} qudit for storing a 'flag' whether this qudit and all 'previous' qudits are in the proper state for acquiring the phase factor: this the way how the ladder type sequences [parts (ii) and (iv)] appear in our construction. As we discuss further, the operation with qudits of type A and C is based on standard schemes of reconstructing multi-qubit controlled gates down to single-qubit and two-qubit gates. At the same time, the implementation of two-qubit operation for qubits in qudits, possessing other uninvolved qubits (qudits of type \mathcal{C}), results in an overhead in the number two-qudit operation (as we discussed in Section IVB2). In order to avoid the doubling of this overhead in the uncomputation, we put the operation with \mathcal{C} type gudits in the middle of our circuit.

However, it is a possibly realizable situation when the number of two-qudit gates required for processing of $\mathcal C$ type qudits is lower than number of two-qudit gates for processing $\mathcal A$ type qudits. In this situation it is preferable to swap $\mathcal A$ and $\mathcal C$ -type qudits in the structure of $\mathrm{circ}_\phi^{\mathrm{qd-int}}$. In order to simplify our description, next we consider processing of original circuit presented in Fig. 8(a). The possible improvement related to swapping $\mathcal A$ and $\mathcal C$ qudits in the structure of $\mathrm{circ}_\phi^{\mathrm{qd-int}}$ is discussed in Appendix B. We also consider modifications of the described scheme in cases where one or two types of qudits are missing (e.g. $|\mathcal B|=0$) in Appendix A.

Below we consider the decomposition of each of the described group of gates to the set of basic single-qudit and two-qudit gates for our transpiler.

a. Processing the multi-controlled gate of Step (i). The idea of its the decomposition is a follows. First, by employing single-qudit rotations $R_{\mathbf{Q}j}^{0,1}(\phi,\theta)$ and $R_{\mathbf{Q}j}^{0,a}(\phi,\theta)$ where $\mathbf{Q}j$ is an affected type- \mathcal{B} qudit, and notations $0 \equiv 0, 1 \equiv d^2 - 1$, and a $0 \equiv 2^{\#j}$ are used, we turn the desired multi-qudit gate into the gate of CZ type [see Fig. 8(b)]. Namely, it adds the phase factor -1 to the state $|\underline{1}\rangle\otimes\ldots\otimes|\underline{1}\rangle$ of the affected qudits, and leaves the remaining states unchanged.

Then we take an ancilla-free decomposition of $(|\mathcal{A}|+1)$ -qubit gate $\mathsf{CZ}_{\mathsf{p0},\ldots,\mathsf{p}(|\mathcal{A}|)}$ gate, acting on abstract qubits $\mathsf{p0},\ldots,\mathsf{p}|\mathcal{A}|$, to single-qubit gates $r_{\mathsf{p}k}(\phi,\theta)$ and two-qubit gates $\mathsf{CZ}_{\mathsf{p}k_1\mathsf{p}k_2}$. This decomposition is used as a 'template' for reconstructing the desired multi-qudit gate into

single-qudit and two-qudit gate. As an example, one can take a standard decomposition from Ref. [67] shown in Fig. 8(d). Next we turn each single qubit gate $r_{\mathsf{p}k}(\phi,\theta)$ into a single-qudit gate $R_{\mathsf{Q}j}^{0,1}(\phi,\theta)$, and each $\mathsf{CZ}_{\mathsf{p}k_1\mathsf{p}k_2}$ into $\mathsf{CZ}_{\mathsf{Q}j_1\mathsf{Q}j_2}^{1,1}$, where the correspondence between qubits $\mathsf{p}0,\ldots,\mathsf{p}|\mathcal{A}|$ and affected qudits is realized via a straightforward ordering (see Fig. 8 (e)). One can see that this construction provides realization of CZ operation in the space spanned by a tensor product of states $|\underline{0}\rangle$ and $|\underline{1}\rangle$ of affected qudits.

We note that it is possible a situation, where the taken qubit-based decomposition of $\mathsf{CZ}_{\mathsf{p0},\dots,\mathsf{p}|\mathcal{A}|}$ realizes the gate up to global phase. In our case, where we embed this decomposition into qudit space, the global phase turns into a relative one between the CZ operation in the subspace spanned by a tensor product of $|\underline{0}\rangle$ and $|\underline{1}\rangle$ states and the identity operation in the remaining subspace. However, this relative phase is removed in the uncomputation Step (v), given that all operation in the uncomputation are Hermitian conjugates of ones in Step (i).

b. Processing the ladder-like sequence on type- \mathcal{B} qudits of Step (ii). Remind that each type- \mathcal{B} qudit has an ancillary level $|a\rangle$ that we use to store the information about whether 'previous' (according to the ordering in Fig. 8(a)) qudits are in the state $|\underline{1}\rangle$. The idea behind employed gates in the ladder-like sequence of Step (ii) is quite straightforward: Each gate turns the state of the target qudit from $|\underline{1}\rangle$ to $|a\rangle$ if and only if the control qudit is in the state $|a\rangle$. One can see that by realizing the sequence of Step (ii), following the Step (i), the last type- \mathcal{B} qudit appears in the state $|a\rangle$ if and only if all type- \mathcal{A} and type- \mathcal{B} qudits were initially the state $|\underline{1}\rangle$. The decomposition of employed in Step (ii) two-qudit gates using native qudit gates can be performed according to schemes of Fig. 8(b) and (c).

c. Processing the multi-controlled of Step (iii). The goal of the considered gate is to acquire the phase factor of -1 to the input state if the last type- \mathcal{B} qudit is in the ancillary state $|a\rangle$, and type- \mathcal{C} gudits are in a such state that all qubits embedded in the type- \mathcal{C} qudits and affected by the decomposed gate are in the state $|1\rangle$. As it was already mentioned, the important point of type- \mathcal{C} qudits is that they also contain unaffected qubits, that results in the fact that the gate of Step (iii) have to acquire the phase factor of -1 to several computational basis states. Specifically, the phase factor of -1 have to acquired to 2^{#unaff} states, where #unaff is a total number of unaffected qubits in type- \mathcal{C} qudits. The intuition behind this fact is exactly the same as behind Eq. (22) of required number of two-qudit gates for realizing an operation between qubits embedded in these gudits.

The idea of decomposing the gate of Step (iii) is very similar to the one of decomposing the gate at Step (i). First, we turn the gate at Step (iii) to a multi-controlled gate of CZ type by adding $R_{\mathbb{Q}j}^{1,a}(\pi/2,\pi)$ and $R_{\mathbb{Q}j}^{1,a}(\pi/2,-\pi)$ rotations on the last qudit $\mathbb{Q}j$ of type \mathcal{B} . Then we take an

ancilla-free decomposition of $(|\mathcal{C}|+1)$ -qubit $\mathsf{CZ}_{\mathsf{p}0,\dots,\mathsf{p}(|\mathcal{C}|)}$ gate (acting on virtual qubits $\mathsf{p}0,\dots,\mathsf{p}|\mathcal{C}|$) to single-qubit rotations $r_{\mathsf{p}k}(\phi,\theta)$ and two-qubit $\mathsf{CZ}_{\mathsf{p}k_1\mathsf{p}k_2}$ gates [see Fig. 7(f)].

Each single-qubit gate $r_{\mathsf{p}k}(\phi,\theta)$ is transformed into the sequence of single-qudit gates

$$\prod_{(\alpha,\beta)} R_{\mathsf{Q}j}^{\alpha,\beta}(\varphi,\theta),\tag{28}$$

where Qj is a qudit corresponding to pk according to the straighforward ordering, and (α, β) are all appropriate level pairs satisfying the condition

$$\begin{aligned} & \operatorname{bin}(\alpha)[\mathsf{pos}] = 0, \operatorname{bin}(\beta)[\mathsf{pos}] = 1, \ \operatorname{for} \ \mathsf{pos} \in \{\mathsf{pos}_\ell\}; \\ & \operatorname{bin}(\alpha)[\mathsf{pos}] = \operatorname{bin}(\beta)[\mathsf{pos}], \ \operatorname{for} \ \mathsf{pos} \notin \{\mathsf{pos}_\ell\}, \end{aligned} \tag{29}$$

and $\{pos_{\ell}\}$ is a set of position of qubits embedded in Qj and affected by the multi-qudit gate of Step (iii).

Two-qubit gates $\mathsf{CZ}_{\mathsf{p}k_1\mathsf{p}k_2}$ are transformed according to Sec. IV B 2. Namely, we take qudits $\mathsf{Q}j_1$ and $\mathsf{Q}j_2$ corresponding to $\mathsf{p}k_1$ and $\mathsf{p}k_2$, chose the set of qubits $\mathsf{q}i_1',\ldots,\mathsf{q}i_\kappa'$ that are embedded in $\mathsf{Q}j_1$ and $\mathsf{Q}j_2$ and are affected by the multi-qudit gate of Step (iii), and transform $\mathsf{CZ}_{\mathsf{q}i_1',\ldots,\mathsf{q}i_\kappa'}$ according to (20) and (21).

In contrast to decomposition of the multi-controlled gate of Step (i), here we should also take into account the global phase factor that may appear from the qubit-based decomposition. Though it is insignificant in the qubit case, when we use this decomposition for qubit embedded into qudits, the phase turns from the global to the relative one (this is the relative phase between the CZ operation in the subspace of affected qubits, and identity operation in the remaining subspace). To compensate this phase in a explicit way, we add a phase single qubit gate

$$\mathsf{Ph}_{\mathsf{p}0}(\gamma) = \begin{bmatrix} e^{\imath\gamma} & 0\\ 0 & e^{\imath\gamma} \end{bmatrix} \tag{30}$$

to the qubit p0. The value of γ is chosen to make the whole sequence of gates, applied to $p0, \ldots, p|\mathcal{C}|$, to realize $\mathsf{CZ}_{p0,\ldots,p|\mathcal{C}|}$ without any global phase.

From the viewpoint of qudit circuit, p0 corresponds to the type- \mathcal{B} qudit Qj involved in the the multi-controlled gate of Step (iii). The qubit phase gate $\mathsf{Ph}_{p0}(\gamma)$ transforms into

$$\mathsf{Ph}^{0}_{\mathsf{Q}_{j}}(\gamma)\mathsf{Ph}^{1}_{\mathsf{Q}_{j}}(\gamma). \tag{31}$$

d. Uncomputation steps (iv) and (v). By its construction, the implementation of Steps (i)-(iii) realizes an acquiring of the phase factor of -1 to such qudits input state, where all embedded qubits affected by the decomposed gate $\mathsf{CZ}_{\mathsf{q1},\ldots,\mathsf{q}\kappa}$ are in state $|1\rangle$. However, we employ ancillary level $|a\rangle$ of type- $\mathcal B$ qudits. To remove the population from $|a\rangle$ to original levels, we employ uncomputation that is a 'mirror refection' of steps (i) and (ii). Namely, the Steps (iv) and (v) are obtained as a

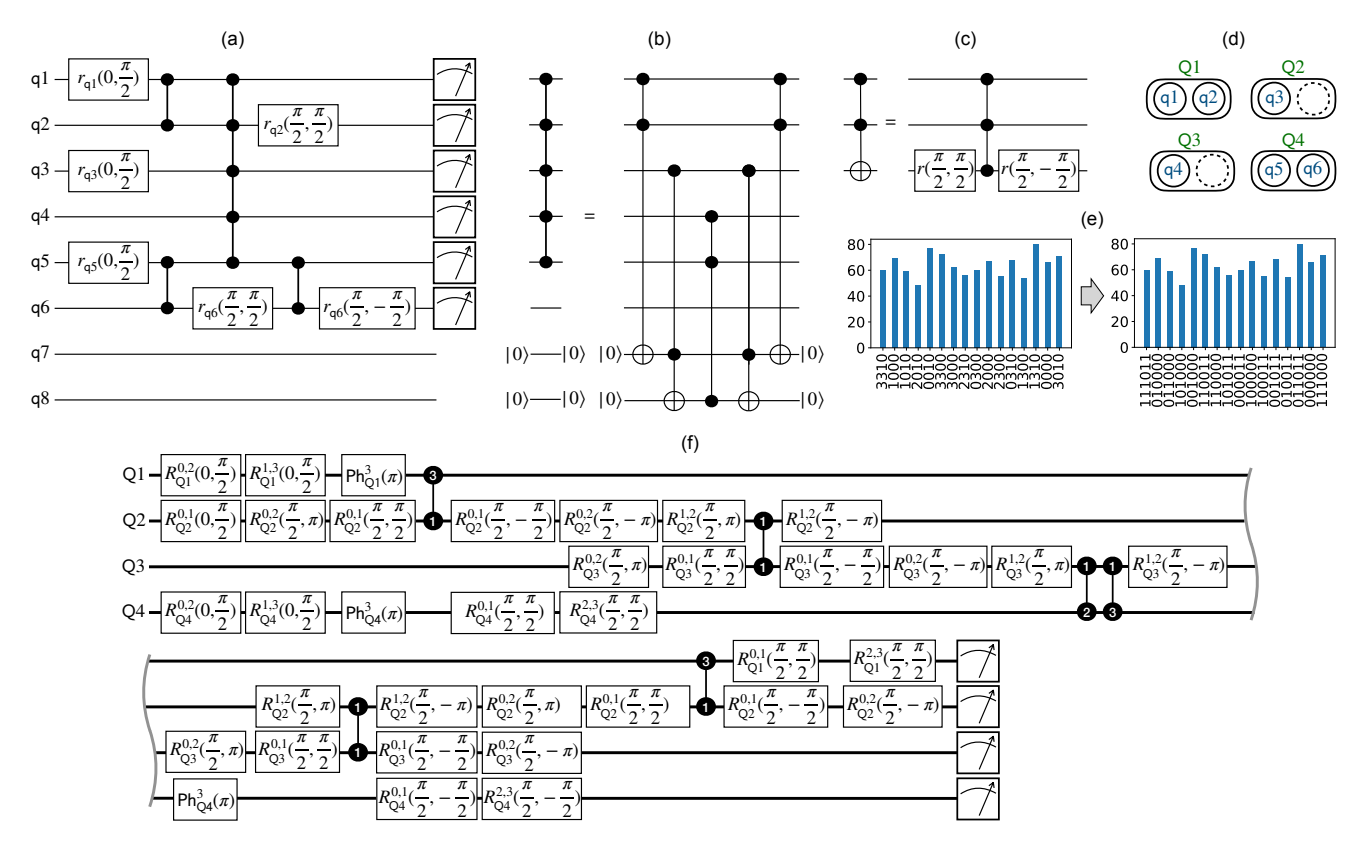


Figure 9. (a) Example of a qubit circuit that is an input to the developed qudit-based transpiler. The circuit acts on n=6 qubits $\mathsf{q1},\ldots,\mathsf{q6}$, two additional qubits $\mathsf{q7},\mathsf{q8}$ are used for decomposing five-qubit $\mathsf{CZ}_{\mathsf{q1},\ldots,\mathsf{q5}}$ gate. (b) Decomposition of five-qubit $\mathsf{CZ}_{\mathsf{q1},\ldots,\mathsf{q5}}$ gate with two 'clean' ancillas down to Toffoli gates. For the decomposition of Toffoli gates the circuit identity shown in (c) and then the scheme of Fig. 8(d) can be used. (d) Qubit-to-qudit mapping that is used for the realization of the given qubit circuit with m=4 qudits of d=4 levels. (e) Equivalence of read-out results that are obtained with qudit-based emulator and post-processed outputs that can be interpreted as results of the qubit circuit implementation. (f) The result of qudit-based traspilation of the input qubit circuit.

Hermitian conjugate of a sequence of steps (i) and (ii): their order is reversed and each $r_{Qj}(\varphi,\theta)$ is transformed to $r_{Qj}(\varphi,-\theta)$ (note that $\mathsf{CZ}_{Qj_1Qj_2} = \mathsf{CZ}_{Qj_1Qj_2}^{\dagger}$). As it was already mentioned, the uncomputation also removes the relative phase between the subspace of affected qubits and remaining subspace of type- \mathcal{A} qudits, possibly acquired in Step (i).

V. REALIZING 6-QUBIT QUANTUM ALGORITHM WITH QUDITS

As an example, we consider the realization of an n=6 qubit circuit, which is presented in Fig. 9(a), with qudit-based processor consisting of m=4 'ququarts' (qudits with d=4). First, let us consider a straightforward implementation of the input circuit with a qubit-based processor. To simplify the transpiration of multi-qubit gate $\mathsf{CZ}_{\mathsf{q1},\ldots,\mathsf{q}6}$, we use two additional ancillary qubits $\mathsf{q7}$, q8. Using schemes shown in Fig. 9(b,c) together with one from Fig. 8(d), $\mathsf{CZ}_{\mathsf{q1},\ldots,\mathsf{q}6}$ can be realized with $5\times 6=30$ two-qubit gates and a number of single-qubit gates. In

this way, the straightforward qubit-based decomposition of the input circuit results in $N_{2\text{-body}}^{\text{qb}} = 33$ two-qubit operations. We note that no restrictions on the coupling map between qubit are considered here.

In contrast, the qubit-to-qudit mapping, shown in Fig. 9(d), allows realizing the input qubit circuit with only $N_{2\text{-body}}^{\text{qd}} = 6$ two-qudit gates. In Fig. 9(e) we show a transformation of 1024 measurement outcomes, obtained with a qudit-based classical emulator, to the read-out measurements outcomes performed in the input qubit circuit. The transpiled qudit circuit is shown in Fig. 9(f). One can see that the qudit-based realization provides an advantage both in the circuit width and depth.

VI. CONCLUSION

We have presented the approach for an efficient implementation of qubit circuits with qudit-based processors. The proposed approach consists of a finding the (sub) optimal qubit-to-qudit mapping, transpiling of a qubit circuit according to to this mapping, running a

transpiled circuit on a qudit-based processor (or emulator), and then reassigning read-out measurement results back to the qubit-based representation. We have developed a qudit-based transpilation algorithm with respect to a particular universal set of single-qudit and two-qudit gates. Then we have shown an an example of applying the developed approach for realizing 6-qubit circuits with four 4-level qudits. Important avenues for future research include the development of an efficient algorithm of finding suboptimal qubit-to-qudit mapping and revealing the role of a native qudit interaction Hamiltonian for qudit-based transpilation process.

ACKNOWLEDGMENTS

The research is supported by the Russian Science Foundation (Grant No. 20-42-05002; qudit-based approach) and Leading Research Center on Quantum Computing (Agreement No. 014/20; implementation of quantum algorithms).

Appendix A: Intermediate circuit in the case of incomplete set of type- $\mathcal{A}, \mathcal{B}, \mathcal{C}$ qudits

While processing multi-qubit gates $\mathsf{CZ}_{\mathsf{q}i_1,\ldots,\mathsf{q}i_\kappa}$ with $|\mathsf{qudit_set}| \geq 3$, it is possible a situation, where one or two types $(\mathcal{A}, \mathcal{B}, \mathcal{C})$ are missing. In this case the described decomposition needs some slight corrections.

If there are no type- \mathcal{B} qudits, then the intermediate circuit consists of a single multi-qudit CZ gate acting on all |qudit_set| qudits. To decompose this gate we take a standard multi-qubit gate decomposition as a template as it is described in Sec. IV B 3 a and IV B 3 c. Then each qubit gate is replaced with corresponding qudit gate(s) taking into account the type of involved qudits (type \mathcal{A} or type \mathcal{C}). The phase correction, discussed in Sec. IV B 3 c, have to be applied if it is necessary.

If there are no type- \mathcal{A} qudits, yet there is at least one type- \mathcal{B} qudit, the ladder-like part of decomposition is started with the control on the first qudit in the state $|\underline{1}\rangle$. If type- \mathcal{C} qudits are also missing, then the ladder-like part of decomposition ends with a target on the last

type \mathcal{B} qudit in the state $|1\rangle$.

Appendix B: Alternative form of the intermediate circuit

The structure of the intermediate qudit circuit $\operatorname{circ}_{\phi}^{\operatorname{qd-int-alt}}$, which is presented in Fig. 10 is similar to the structure of the previously described $\operatorname{circ}_{\phi}^{\operatorname{qd-int}}$. The main difference between them is location of type $\mathcal A$ and $\mathcal C$ qudits in the scheme. In the alternative version multi-qudit gate on type- $\mathcal C$ qudits is employed twice and multi-qudit gate on type $\mathcal A$ is employed once in the central part of the scheme. We note that operations on type $\mathcal B$ qudits remain the same as in the previously described scheme in Fig. 8(a).

Taking into account invariability of operations on type $\mathcal B$ qudits and the symmetry of CZ type operation in the core of type- $\mathcal A$ and $\mathcal C$ multi-qudit gates, realization of the CZ type operation on $\mathcal A$ and $\mathcal C$ qudits reduces to the procedures described in Sections IV B 3 a and IV B 3 c, correspondingly.

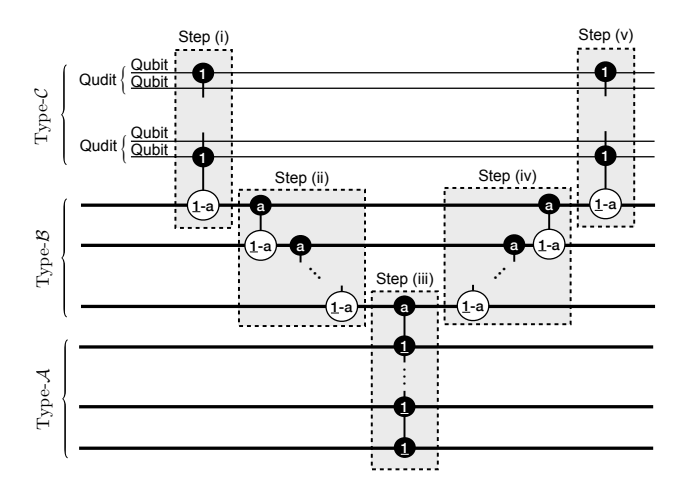


Figure 10. Alternative intermediate qudit circuit $\operatorname{circ}_{\phi}^{\operatorname{qd-int-alt}}$ for the decomposition of $\operatorname{CZ}_{\mathfrak{q}i_1,\ldots,\mathfrak{q}i_\kappa}$ gate. The difference from the described in the main text scheme (see Fig. 8) is the locations of swapping operations of type- \mathcal{A} and type- \mathcal{C} qudits.

H. Bernien, S. Schwartz, A. Keesling, H. Levine, A. Omran, H. Pichler, S. Choi, A. S. Zibrov, M. Endres, M. Greiner, V. Vuletić, and M. D. Lukin, Nature 551, 579 (2017).

^[2] S. Ebadi, T. T. Wang, H. Levine, A. Keesling, G. Semeghini, A. Omran, D. Bluvstein, R. Samajdar, H. Pichler, W. W. Ho, S. Choi, S. Sachdev, M. Greiner, V. Vuletić, and M. D. Lukin, Nature 595, 227 (2021).

^[3] J. Zhang, G. Pagano, P. W. Hess, A. Kyprianidis, P. Becker, H. Kaplan, A. V. Gorshkov, Z. X. Gong, and C. Monroe, Nature 551, 601 (2017).

^[4] D. Barredo, V. Lienhard, S. de Léséleuc, T. Lahaye, and A. Browaeys, Nature 561, 79 (2018).

^[5] F. Arute, K. Arya, R. Babbush, D. Bacon, J. C. Bardin, R. Barends, R. Biswas, S. Boixo, F. G. S. L. Brandao, D. A. Buell, B. Burkett, Y. Chen, Z. Chen, B. Chiaro, R. Collins, W. Courtney, A. Dunsworth, E. Farhi, B. Foxen, A. Fowler, C. Gidney, M. Giustina, R. Graff, K. Guerin, S. Habegger, M. P. Harrigan, M. J. Hartmann, A. Ho, M. Hoffmann, T. Huang, T. S. Humble, S. V. Isakov, E. Jeffrey, Z. Jiang, D. Kafri, K. Kechedzhi, J. Kelly, P. V. Klimov, S. Knysh,

- A. Korotkov, F. Kostritsa, D. Landhuis, M. Lindmark, E. Lucero, D. Lyakh, S. Mandrà, J. R. McClean, M. McEwen, A. Megrant, X. Mi, K. Michielsen, M. Mohseni, J. Mutus, O. Naaman, M. Neeley, C. Neill, M. Y. Niu, E. Ostby, A. Petukhov, J. C. Platt, C. Quintana, E. G. Rieffel, P. Roushan, N. C. Rubin, D. Sank, K. J. Satzinger, V. Smelyanskiy, K. J. Sung, M. D. Trevithick, A. Vainsencher, B. Villalonga, T. White, Z. J. Yao, P. Yeh, A. Zalcman, H. Neven, and J. M. Martinis, Nature 574, 505 (2019).
- [6] N. Friis, O. Marty, C. Maier, C. Hempel, M. Holzäpfel, P. Jurcevic, M. B. Plenio, M. Huber, C. Roos, R. Blatt, and B. Lanyon, Phys. Rev. X 8, 021012 (2018).
- [7] P. J. J. O'Malley, R. Babbush, I. D. Kivlichan, J. Romero, J. R. McClean, R. Barends, J. Kelly, P. Roushan, A. Tranter, N. Ding, B. Campbell, Y. Chen, Z. Chen, B. Chiaro, A. Dunsworth, A. G. Fowler, E. Jeffrey, E. Lucero, A. Megrant, J. Y. Mutus, M. Neeley, C. Neill, C. Quintana, D. Sank, A. Vainsencher, J. Wenner, T. C. White, P. V. Coveney, P. J. Love, H. Neven, A. Aspuru-Guzik, and J. M. Martinis, Phys. Rev. X 6, 031007 (2016).
- [8] A. Kandala, A. Mezzacapo, K. Temme, M. Takita, M. Brink, J. M. Chow, and J. M. Gambetta, Nature 549, 242 (2017).
- [9] C. Hempel, C. Maier, J. Romero, J. McClean, T. Monz, H. Shen, P. Jurcevic, B. P. Lanyon, P. Love, R. Babbush, A. Aspuru-Guzik, R. Blatt, and C. F. Roos, Phys. Rev. X 8, 031022 (2018).
- [10] N. Moll, P. Barkoutsos, L. S. Bishop, J. M. Chow, A. Cross, D. J. Egger, S. Filipp, A. Fuhrer, J. M. Gambetta, M. Ganzhorn, A. Kandala, A. Mezzacapo, P. Müller, W. Riess, G. Salis, J. Smolin, I. Tavernelli, and K. Temme, Quantum Science and Technology 3, 030503 (2018).
- [11] X. Xue, M. Russ, N. Samkharadze, B. Undseth, A. Sam-mak, G. Scappucci, and L. M. K. Vandersypen, Nature 601, 343 (2022).
- [12] M. T. Madzik, S. Asaad, A. Youssry, B. Joecker, K. M. Rudinger, E. Nielsen, K. C. Young, T. J. Proctor, A. D. Baczewski, A. Laucht, V. Schmitt, F. E. Hudson, K. M. Itoh, A. M. Jakob, B. C. Johnson, D. N. Jamieson, A. S. Dzurak, C. Ferrie, R. Blume-Kohout, and A. Morello, Nature 601, 348 (2022).
- [13] A. Noiri, K. Takeda, T. Nakajima, T. Kobayashi, A. Sam-mak, G. Scappucci, and S. Tarucha, Nature 601, 338 (2022).
- [14] H.-S. Zhong, H. Wang, Y.-H. Deng, M.-C. Chen, L.-C. Peng, Y.-H. Luo, J. Qin, D. Wu, X. Ding, Y. Hu, P. Hu, X.-Y. Yang, W.-J. Zhang, H. Li, Y. Li, X. Jiang, L. Gan, G. Yang, L. You, Z. Wang, L. Li, N.-L. Liu, C.-Y. Lu, and J.-W. Pan, Science 370, 1460 (2020).
- [15] L. S. Madsen, F. Laudenbach, M. F. Askarani, F. Rortais, T. Vincent, J. F. F. Bulmer, F. M. Miatto, L. Neuhaus, L. G. Helt, M. J. Collins, A. E. Lita, T. Gerrits, S. W. Nam, V. D. Vaidya, M. Menotti, I. Dhand, Z. Vernon, N. Quesada, and J. Lavoie, Nature 606, 75 (2022).
- [16] E. Moreno-Pineda, C. Godfrin, F. Balestro, W. Wernsdorfer, and M. Ruben, Chem. Soc. Rev. 47, 501 (2018).
- [17] M. Erhard, R. Fickler, M. Krenn, and A. Zeilinger, Light: Science & Applications 7, 17146 (2018).
- [18] E. Farhi and S. Gutmann, Phys. Rev. A 57, 2403 (1998).
- [19] A. R. Kessel' and V. L. Ermakov, Journal of Experimental and Theoretical Physics Letters 70, 61 (1999).

- [20] A. R. Kessel' and V. L. Ermakov, Journal of Experimental and Theoretical Physics Letters 71, 307 (2000).
- [21] A. R. Kessel and N. M. Yakovleva, Phys. Rev. A 66, 062322 (2002).
- [22] A. Muthukrishnan and C. R. Stroud, Phys. Rev. A 62, 052309 (2000).
- [23] M. A. Nielsen, M. J. Bremner, J. L. Dodd, A. M. Childs, and C. M. Dawson, Phys. Rev. A 66, 022317 (2002).
- [24] X. Wang, B. C. Sanders, and D. W. Berry, Phys. Rev. A 67, 042323 (2003).
- [25] A. B. Klimov, R. Guzmán, J. C. Retamal, and C. Saave-dra, Phys. Rev. A 67, 062313 (2003).
- [26] E. Bagan, M. Baig, and R. Muñoz Tapia, Phys. Rev. A 67, 014303 (2003).
- [27] A. Y. Vlasov, in First International Symposium on Quantum Informatics, Vol. 5128, edited by Y. I. Ozhigov, International Society for Optics and Photonics (SPIE, 2003) pp. 29 36.
- [28] A. D. Greentree, S. G. Schirmer, F. Green, L. C. L. Hollenberg, A. R. Hamilton, and R. G. Clark, Phys. Rev. Lett. 92, 097901 (2004).
- [29] D. P. O'Leary, G. K. Brennen, and S. S. Bullock, Phys. Rev. A 74, 032334 (2006).
- [30] T. C. Ralph, K. J. Resch, and A. Gilchrist, Phys. Rev. A 75, 022313 (2007).
- [31] B. P. Lanyon, T. J. Weinhold, N. K. Langford, J. L. O'Brien, K. J. Resch, A. Gilchrist, and A. G. White, Phys. Rev. Lett. 100, 060504 (2008).
- [32] R. Ionicioiu, T. P. Spiller, and W. J. Munro, Phys. Rev. A 80, 012312 (2009).
- [33] S. S. Ivanov, H. S. Tonchev, and N. V. Vitanov, Phys. Rev. A 85, 062321 (2012).
- [34] B. Li, Z.-H. Yu, and S.-M. Fei, Scientific Reports 3, 2594 (2013).
- [35] E. O. Kiktenko, A. K. Fedorov, O. V. Man'ko, and V. I. Man'ko, Phys. Rev. A 91, 042312 (2015).
- [36] E. Kiktenko, A. Fedorov, A. Strakhov, and V. Man'ko, Physics Letters A 379, 1409 (2015).
- [37] C. Song, S.-L. Su, J.-L. Wu, D.-Y. Wang, X. Ji, and S. Zhang, Phys. Rev. A 93, 062321 (2016).
- [38] A. Frydryszak, L. Jakóbczyk, and P. Lugiewicz, Journal of Physics: Conference Series 804, 012016 (2017).
- [39] A. Bocharov, M. Roetteler, and K. M. Svore, Phys. Rev. A 96, 012306 (2017).
- [40] P. Gokhale, J. M. Baker, C. Duckering, N. C. Brown, K. R. Brown, and F. T. Chong, in *Proceedings of the* 46th International Symposium on Computer Architecture, ISCA '19 (Association for Computing Machinery, New York, NY, USA, 2019) pp. 554–566.
- [41] Y.-H. Luo, H.-S. Zhong, M. Erhard, X.-L. Wang, L.-C. Peng, M. Krenn, X. Jiang, L. Li, N.-L. Liu, C.-Y. Lu, A. Zeilinger, and J.-W. Pan, Phys. Rev. Lett. 123, 070505 (2019).
- [42] P. J. Low, B. M. White, A. A. Cox, M. L. Day, and C. Senko, Phys. Rev. Research 2, 033128 (2020).
- [43] Z. Jin, W.-J. Gong, A.-D. Zhu, S. Zhang, Y. Qi, and S.-L. Su, Opt. Express 29, 10117 (2021).
- [44] M. Neeley, M. Ansmann, R. C. Bialczak, M. Hofheinz, E. Lucero, A. D. O'Connell, D. Sank, H. Wang, J. Wenner, A. N. Cleland, M. R. Geller, and J. M. Martinis, Science 325, 722 (2009).
- [45] B. P. Lanyon, M. Barbieri, M. P. Almeida, T. Jennewein, T. C. Ralph, K. J. Resch, G. J. Pryde, J. L. O'Brien, A. Gilchrist, and A. G. White, Nature Physics 5, 134

- (2009).
- [46] A. Fedorov, L. Steffen, M. Baur, M. P. da Silva, and A. Wallraff, Nature 481, 170 (2012).
- [47] B. E. Mischuck, S. T. Merkel, and I. H. Deutsch, Phys. Rev. A 85, 022302 (2012).
- [48] M. J. Peterer, S. J. Bader, X. Jin, F. Yan, A. Kamal, T. J. Gudmundsen, P. J. Leek, T. P. Orlando, W. D. Oliver, and S. Gustavsson, Phys. Rev. Lett. 114, 010501 (2015).
- [49] E. Svetitsky, H. Suchowski, R. Resh, Y. Shalibo, J. M. Martinis, and N. Katz, Nature Communications 5, 5617 (2014).
- [50] J. Braumüller, J. Cramer, S. Schlör, H. Rotzinger, L. Radtke, A. Lukashenko, P. Yang, S. T. Skacel, S. Probst, M. Marthaler, L. Guo, A. V. Ustinov, and M. Weides, Phys. Rev. B 91, 054523 (2015).
- [51] M. Kues, C. Reimer, P. Roztocki, L. R. Cortés, S. Sciara, B. Wetzel, Y. Zhang, A. Cino, S. T. Chu, B. E. Little, D. J. Moss, L. Caspani, J. Azaña, and R. Morandotti, Nature 546, 622 (2017).
- [52] C. Godfrin, A. Ferhat, R. Ballou, S. Klyatskaya, M. Ruben, W. Wernsdorfer, and F. Balestro, Phys. Rev. Lett. 119, 187702 (2017).
- [53] R. Sawant, J. A. Blackmore, P. D. Gregory, J. Mur-Petit, D. Jaksch, J. Aldegunde, J. M. Hutson, M. R. Tarbutt, and S. L. Cornish, New Journal of Physics 22, 013027 (2020).
- [54] A. Pavlidis and E. Floratos, Phys. Rev. A 103, 032417 (2021).
- [55] P. Rambow and M. Tian, "Reduction of circuit depth by mapping qubit-based quantum gates to a qudit basis," (2021).
- [56] M. Ringbauer, M. Meth, L. Postler, R. Stricker, R. Blatt, P. Schindler, and T. Monz, "A universal qudit quantum processor with trapped ions," (2021).

- [57] A. D. Hill, M. J. Hodson, N. Didier, and M. J. Reagor, "Realization of arbitrary doubly-controlled quantum phase gates," (2021).
- [58] Y. Chi, J. Huang, Z. Zhang, J. Mao, Z. Zhou, X. Chen, C. Zhai, J. Bao, T. Dai, H. Yuan, M. Zhang, D. Dai, B. Tang, Y. Yang, Z. Li, Y. Ding, L. K. Oxenløwe, M. G. Thompson, J. L. O'Brien, Y. Li, Q. Gong, and J. Wang, Nature Communications 13, 1166 (2022).
- [59] E. O. Kiktenko, A. S. Nikolaeva, P. Xu, G. V. Shlyapnikov, and A. K. Fedorov, Phys. Rev. A 101, 022304 (2020).
- [60] A. S. Nikolaeva, E. O. Kiktenko, and A. K. Fedorov, Phys. Rev. A 105, 032621 (2022).
- [61] A. Galda, M. Cubeddu, N. Kanazawa, P. Narang, and N. Earnest-Noble, "Implementing a ternary decomposition of the toffoli gate on fixed-frequency transmon qutrits," (2021).
- [62] X. Gu, J. Allcock, S. An, and Y.-x. Liu, "Efficient multiqubit subspace rotations via topological quantum walks," (2021).
- [63] F. T. Chong, D. Franklin, and M. Martonosi, Nature 549, 180 (2017).
- [64] D. Zhu, Z.-P. Cian, C. Noel, A. Risinger, D. Biswas, L. Egan, Y. Zhu, A. M. Green, C. H. Alderete, N. H. Nguyen, Q. Wang, A. Maksymov, Y. Nam, M. Cetina, N. M. Linke, M. Hafezi, and C. Monroe, "Crossplatform comparison of arbitrary quantum computations," (2021).
- [65] N. Earnest, C. Tornow, and D. J. Egger, Phys. Rev. Research 3, 043088 (2021).
- [66] D. P. DiVincenzo, Fortschritte der Physik 48, 771 (2000).
- [67] A. Barenco, C. H. Bennett, R. Cleve, D. P. DiVincenzo, N. Margolus, P. Shor, T. Sleator, J. A. Smolin, and H. Weinfurter, Phys. Rev. A 52, 3457 (1995).